

standard deviations are variance weighted. Rhythmic traces are those with any period estimate in the circadian range, 15–35 h, as described⁸. All rhythm assays were conducted at 22 °C.

Received 9 April; accepted 13 June 2002; doi:10.1038/nature00954.

1. Thomas, B. & Vince-Prue, D. *Photoperiodism in Plants* (Academic, San Diego, 1997).
2. Carré, I. A. Day-length perception and the photoperiodic regulation of flowering in *Arabidopsis*. *J. Biol. Rhythms* **16**, 416–424 (2001).
3. Alabadi, D. *et al.* Reciprocal regulation between *TOC1* and *LHY/CCA1* within the *Arabidopsis* circadian clock. *Science* **293**, 880–883 (2001).
4. Wang, Z. & Tobin, E. M. Constitutive expression of the *CIRCADIAN CLOCK ASSOCIATED 1 (CCA1)* gene disrupts circadian rhythms and suppresses its own expression. *Cell* **93**, 1207–1217 (1998).
5. Putterill, J., Robson, F., Lee, K., Simon, R. & Coupland, G. The *CONSTANS* gene of *Arabidopsis* promotes flowering and encodes a protein showing similarities to zinc finger transcription factors. *Cell* **80**, 847–857 (1995).
6. Koornneef, M., Hanhart, C. J. & van der Veen, J. H. A genetic and physiological analysis of late flowering mutants in *Arabidopsis thaliana*. *Mol. Gen. Genet.* **229**, 57–66 (1991).
7. Samach, A. & Coupland, G. Time measurement and the control of flowering in plants. *BioEssays* **22**, 38–47 (2000).
8. Dowson-Day, M. J. & Millar, A. J. Circadian dysfunction causes aberrant hypocotyl elongation patterns in *Arabidopsis*. *Plant J.* **17**, 63–71 (1999).
9. Hicks, K. A. *et al.* Conditional circadian dysfunction of the *Arabidopsis early-flowering 3* mutant. *Science* **274**, 790–792 (1996).
10. Zagotta, M. T. *et al.* The *Arabidopsis ELF3* gene regulates vegetative photomorphogenesis and the photoperiodic induction of flowering. *Plant J.* **10**, 691–702 (1996).
11. McWatters, H. G., Bastow, R. M., Hall, A. & Millar, A. J. The *ELF3* zeitnehmer regulates light signalling to the circadian clock. *Nature* **408**, 716–720 (2000).
12. Liu, X. L., Covington, M. F., Fankhauser, C., Chory, J. & Wagner, D. R. *ELF3* encodes a circadian clock-regulated nuclear protein that functions in an *Arabidopsis* PHYB signal transduction pathway. *Plant Cell* **13**, 1293–1304 (2001).
13. Covington, M. F. *et al.* *ELF3* modulates resetting of the circadian clock in *Arabidopsis*. *Plant Cell* **13**, 1305–1315 (2001).
14. Hicks, K. A., Albertson, T. M. & Wagner, D. R. *EARLY FLOWERING 3* encodes a novel protein that regulates circadian clock function and flowering in *Arabidopsis*. *Plant Cell* **13**, 1281–1292 (2001).
15. Reed, J. W. *et al.* Independent action of *ELF3* and *phyB* to control hypocotyl elongation and flowering time. *Plant Physiol.* **122**, 1149–1160 (2000).
16. Bell-Pedersen, D., Crosthwaite, S. K., Lakin-Thomas, P. L., Mellow, M. & Okland, M. The Neurospora circadian clock: simple or complex? *Phil. Trans. R. Soc. Lond. B* **356**, 1697–1709 (2001).
17. Aronson, B. D., Johnson, K. A. & Dunlap, J. C. Circadian clock locus frequency: protein encoded by a single open reading frame defines period length and temperature compensation. *Proc. Natl Acad. Sci. USA* **91**, 7683–7687 (1994).
18. Strayer, C. *et al.* Cloning of the *Arabidopsis* clock gene *TOC1*, an autoregulatory response regulator homolog. *Science* **289**, 768–771 (2000).
19. Feldmann, K. A. T-DNA insertion mutagenesis in *Arabidopsis*: mutational spectrum. *Plant J.* **1**, 71–82 (1991).
20. Onouchi, H., Igeno, M. I., Perilleux, C., Graves, K. & Coupland, G. Mutagenesis of plants overexpressing *CONSTANS* demonstrates novel interactions among *Arabidopsis* flowering-time genes. *Plant Cell* **12**, 885–900 (2000).
21. Suarez-Lopez, P. *et al.* *CONSTANS* mediates between the circadian clock and the control of flowering in *Arabidopsis*. *Nature* **410**, 1116–1120 (2001).
22. Davis, S. J., Bhoo, S. H., Durski, A. M., Walker, J. M. & Vierstra, R. D. The heme-oxygenase family required for phytochrome chromophore biosynthesis is necessary for proper photomorphogenesis in higher plants. *Plant Physiol.* **126**, 656–669 (2001).
23. Kardailsky, I. *et al.* Activation tagging of the floral inducer *FT*. *Science* **286**, 1962–1965 (1999).
24. Bognar, L. K. *et al.* The circadian clock controls the expression pattern of the circadian input photoreceptor, phytochrome B. *Proc. Natl Acad. Sci. USA* **96**, 14652–14657 (1999).
25. Carré, I. A. & Kay, S. A. Multiple DNA–protein complexes at a circadian-regulated promoter element. *Plant Cell* **7**, 2039–2051 (1995).

Supplementary Information accompanies the paper on Nature's website (<http://www.nature.com/nature>).

Acknowledgements

This work was supported by the College of Agricultural and Life Sciences of the University of Wisconsin and by a grant to R.A. from the National Science Foundation. M.R.D. was supported by a Molecular Biosciences Training Grant (NIH); R.M.B. was supported by a Gatsby graduate studentship; S.J.D. is a Department of Energy Bioscience fellow of the Life Sciences Research Foundation. Work in Warwick was supported by grants from the Biotechnology and Biological Sciences Research Council and the Human Frontier Science Program (HFSP) to A.J.M. The work in Hungary was supported by the Howard Hughes Medical Institute.

Competing interests statement

The authors declare that they have no competing financial interests.

Correspondence and requests for materials should be addressed to R.M.A. (e-mail: amasino@biochem.wisc.edu) or A.J.M. (e-mail: Andrew.Millar@warwick.ac.uk). The accession code for *ELF4* is AY035183.

.....
Protective role of phospholipid oxidation products in endotoxin-induced tissue damage

Valery N. Bochkov, Alexandra Kadl, Joakim Huber, Florian Gruber, Bernd R. Binder & Norbert Leitinger

Department of Vascular Biology and Thrombosis Research, University of Vienna, Schwarzschanerstrasse 17, 1090 Vienna, Austria; and BMT-Research, Brunnerstrasse 59/5, 1235 Vienna, Austria

Lipopolysaccharide (LPS), an outer-membrane component of Gram-negative bacteria, interacts with LPS-binding protein and CD14, which present LPS to toll-like receptor 4 (refs 1, 2), which activates inflammatory gene expression through nuclear factor κ B (NF κ B) and mitogen-activated protein-kinase signalling^{3,4}. Antibacterial defence involves activation of neutrophils that generate reactive oxygen species capable of killing bacteria⁵; therefore host lipid peroxidation occurs, initiated by enzymes such as NADPH oxidase and myeloperoxidase⁶. Oxidized phospholipids are pro-inflammatory agonists promoting chronic inflammation in atherosclerosis⁷; however, recent data suggest that they can inhibit expression of inflammatory adhesion molecules⁸. Here we show that oxidized phospholipids inhibit LPS-induced but not tumour-necrosis factor- α -induced or interleukin-1 β -induced NF κ B-mediated upregulation of inflammatory genes, by blocking the interaction of LPS with LPS-binding protein and CD14. Moreover, in LPS-injected mice, oxidized phospholipids inhibited inflammation and protected mice from lethal endotoxin shock. Thus, in severe Gram-negative bacterial infection, endogenously formed oxidized phospholipids may function as a negative feedback to blunt innate immune responses. Furthermore, identified chemical structures capable of inhibiting the effects of endotoxins such as LPS could be used for the development of new drugs for treatment of sepsis.

Lipids containing polyunsaturated fatty acids such as 1-palmitoyl-2-arachidonoyl-*sn*-glycero-3-phosphorylcholine (PAPC) are especially prone to oxidative modification. Oxidation of PAPC results in generation of a mixture of oxidation products (OxPAPC), some of which stimulate adhesion of monocytes to endothelial cells and induce expression of inflammatory genes in endothelial cells^{8–10}. Thus, a role for oxidized phospholipids as culprits in chronic inflammation was suggested. On the other hand, we have shown that OxPAPC inhibited neutrophil adhesion to endothelial cells induced by LPS⁸.

Here we show that OxPAPC blocked LPS-induced upregulation of the inflammatory adhesion molecules E-selectin, ICAM-1 and VCAM-1 on human umbilical-vein endothelial cells (HUVEC) (Fig. 1a). The inhibitory effect of OxPAPC was concentration-dependent, with half-maximal inhibition observed at 10 μ g ml⁻¹ OxPAPC (Fig. 1b). The effects of LPS at concentrations as high as 500 ng ml⁻¹ were inhibited by 50 μ g ml⁻¹ OxPAPC. Because expression of E-selectin, ICAM-1 and VCAM-1 is NF κ B-dependent, we examined the influence of OxPAPC on signalling events at different levels of the NF κ B cascade. We found that OxPAPC inhibited LPS-induced activation of a 5 \times NF κ B-luciferase reporter construct (Fig. 1c), binding of p65 to its DNA consensus site (Fig. 1d), and phosphorylation and degradation of I κ B α (Fig. 1e).

NF κ B is activated during inflammation by various receptors including the LPS toll-like receptor 4 (TLR4), the interleukin 1 (IL-1) receptor, and the tumour-necrosis factor- α (TNF α) receptor. In contrast to LPS, TNF α -induced phosphorylation and degra-

dation of I κ B α were not significantly inhibited by OxPAPC (Fig. 1e). Moreover, OxPAPC blocked LPS-induced but not TNF α -induced activation of p38 mitogen-activated protein (MAP) kinase (Fig. 1e). Signalling events downstream of the IL-1 receptor and TLR4 converge on MyD88, which binds to the cytosolic domains of the receptors and couples them to downstream signalling cascades⁴. However, effects of IL-1 β on expression of E-selectin were not inhibited by OxPAPC (Fig. 1f). Thus, these data indicate that the inhibitory effect of OxPAPC was specific for LPS and occurred upstream of MyD88, apparently at the level of LPS recognition by cellular or soluble receptor(s).

Activation of innate immune responses by LPS can be inhibited by various soluble molecules that bind LPS and neutralize its activity. These include certain plasma proteins, lipoproteins and lipids^{11–14} and inhibitors structurally related to polymyxin B¹⁵. Alternatively, the action of LPS is inhibited by lipid-A-like LPS antagonists, which form inactive complexes with TLR4 or its accessory proteins¹⁶. Both the inhibitory action of LPS-binding substances as well as lipid-A-like LPS antagonists can be overcome

by high LPS concentrations¹⁷. We found, however, that increasing LPS concentrations could not overcome the inhibitory effect of OxPAPC (Fig. 2a). Moreover, LPS-trapping substances are known to inhibit LPS-induced clotting activity of the *Limulus* amoebocyte lysate (LAL), while several lipid-A-like LPS antagonists activate clotting¹⁸. OxPAPC neither stimulated nor inhibited LPS-induced clotting activity of the LAL (Fig. 2b). Although serum also contains LPS-binding activity, increasing concentrations of serum did not mimic the inhibitory action of OxPAPC on E-selectin expression induced by LPS (Fig. 2c). These data indicate that OxPAPC inhibits LPS action by a mechanism different from known LPS antagonists. We hypothesized that OxPAPC could interfere with recognition of LPS by LPS-binding protein (LBP) and CD14, both presenting LPS to TLR4 (ref. 2)

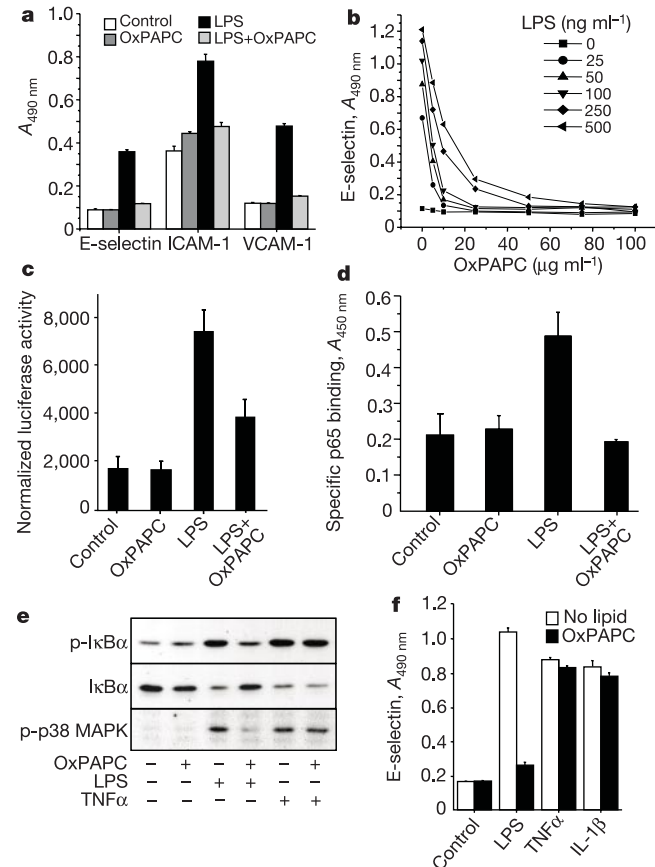


Figure 1 OxPAPC selectively inhibits LPS-induced intracellular signalling and expression of inflammatory adhesion molecules in HUVEC. **a**, OxPAPC inhibits LPS-induced upregulation of E-selectin, ICAM-1 and VCAM-1. **b**, The inhibitory effect of OxPAPC on LPS-induced E-selectin expression is concentration-dependent. **c**, OxPAPC inhibits LPS-induced activation of a $5 \times$ NF κ B–luciferase reporter. **d**, OxPAPC inhibits LPS-induced DNA-binding activity of p65. ‘Specific’ binding represents the difference between the binding in the absence or presence of excess of soluble consensus oligonucleotide. **e**, OxPAPC blocks LPS-induced phosphorylation (p) and degradation of I κ B α and p38 MAP kinase phosphorylation. **f**, OxPAPC inhibits the action of LPS, but not of IL-1 β and TNF α . HUVEC were stimulated with LPS (300 ng ml^{-1}), TNF α (20 U ml^{-1}) or IL-1 β (10 ng ml^{-1}) in the presence or absence of $50 \text{ } \mu\text{g ml}^{-1}$ OxPAPC. **a–f**, See Methods for additional experimental details. $A_{490 \text{ nm}}$, absorbance at 490 nm.

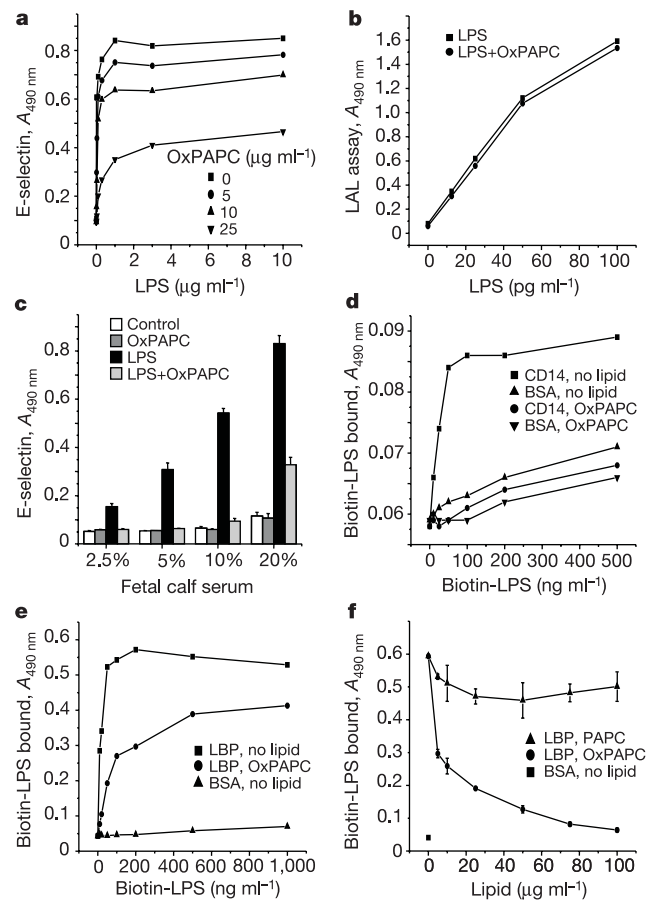


Figure 2 OxPAPC inhibits effects of LPS by blocking interactions of LPS with LBP and CD14. **a**, Increasing concentrations of LPS do not overcome the inhibitory activity of OxPAPC. HUVEC were stimulated with increasing concentrations of LPS in the presence of indicated concentrations of OxPAPC. E-selectin ELISA was performed as described in Methods. **b**, OxPAPC does not interfere with the LAL endotoxin assay. **c**, LPS-induced expression of E-selectin is not inhibited by high concentrations of serum. HUVEC were stimulated with LPS in the presence or absence of OxPAPC in medium 199 supplemented with indicated concentrations of bovine calf serum. **d**, OxPAPC inhibits binding of biotin-LPS to immobilized CD14. Binding and detection of biotinylated LPS to CD14- or BSA-coated microwell plates were performed as described in the Methods. Where indicated, the incubation medium contained $50 \text{ } \mu\text{g ml}^{-1}$ OxPAPC. **e**, OxPAPC inhibits binding of biotin-LPS to immobilized LBP. **f**, Concentration dependence of the inhibition of LPS/LBP binding by OxPAPC. Microwells containing immobilized LBP were treated with indicated concentrations of sonicated native or oxidized PAPC and 100 ng ml^{-1} biotin-LPS. Detection of bound biotin-LPS was performed as described in Methods.

and being critical for LPS signalling in endothelial cells^{19,20}. Apart from LPS, CD14 and LBP have been shown to bind phospholipids catalysing their transfer between cells and lipoproteins^{21,22}. Indeed, OxPAPC inhibited binding of LPS to immobilized CD14 (Fig. 2d). OxPAPC also inhibited binding of LPS to immobilized LBP (Fig. 2e). The inhibitory action was concentration-dependent

and specific for oxidized PAPC, whereas native PAPC was not effective (Fig. 2f).

Next we examined structural requirements for lipids to inhibit effects of LPS. We found that the inhibitory activity was specific for oxidized phospholipids because other lipids that are potentially present in OxPAPC preparations and known to exert a variety of

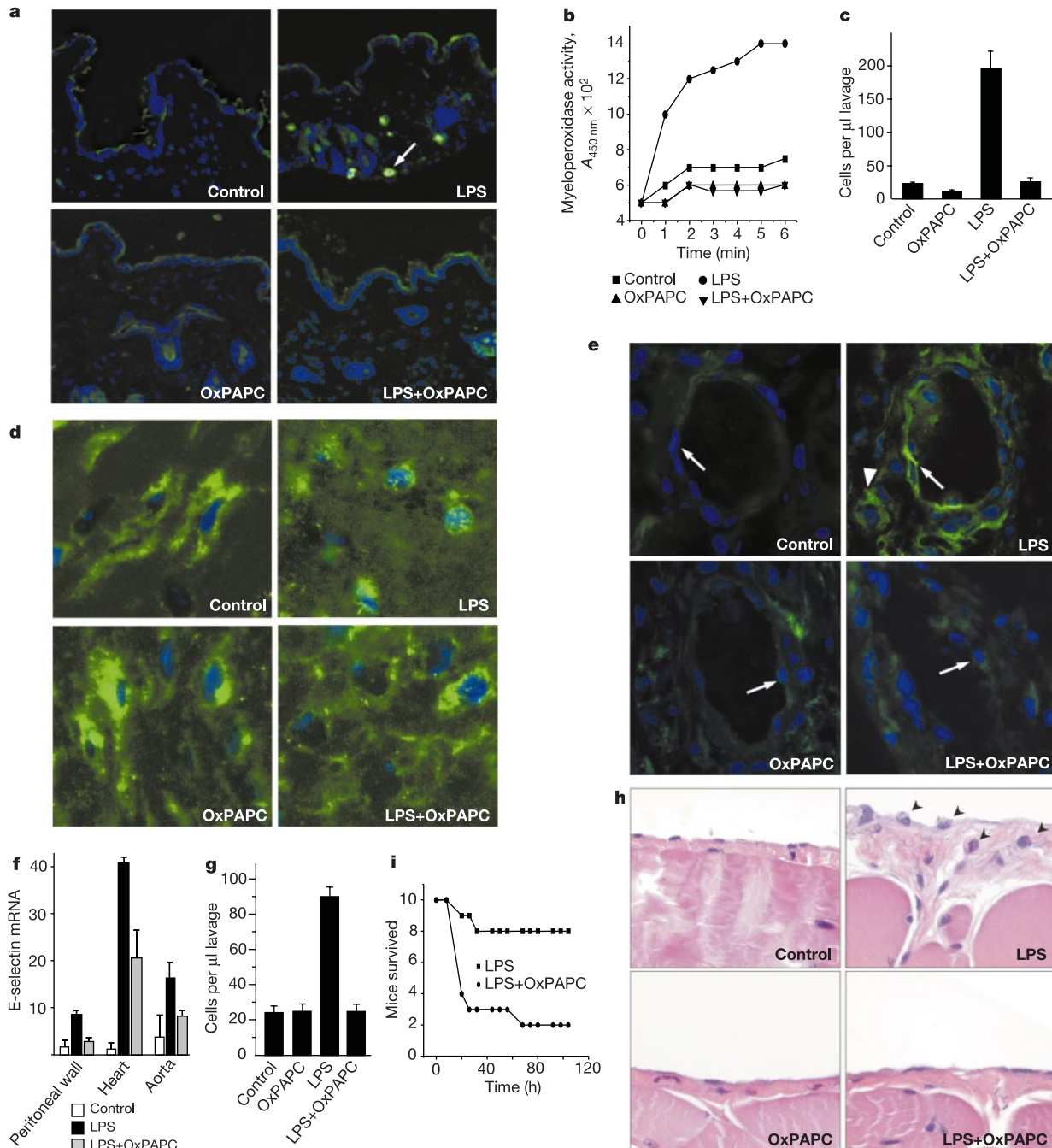


Figure 3 Oxidized phospholipids inhibit effects of endotoxin *in vivo*. **a**, OxPAPC inhibits LPS-induced accumulation of leukocytes reactive for myeloperoxidase in mouse skin. Arrow indicates myeloperoxidase-expressing leukocyte. **b**, Myeloperoxidase activity in the skin of LPS/OxPAPC-treated mice. **c**, OxPAPC inhibits LPS-induced accumulation of leukocytes in the air pouch model of inflammation. **d**, OxPAPC inhibits LPS-induced nuclear translocation of p65 in the air pouch wall. We note colocalization of p65 (green) with DAPI-stained nuclei (blue) in LPS-treated cells. **e**, OxPAPC inhibits LPS-induced VCAM-1 expression in the air pouch wall. Arrow indicates endothelial cell, arrowhead indicates myofibroblasts of the pouch wall. **f**, OxPAPC inhibits induction of E-selectin

mRNA by LPS. Expression of E-selectin mRNA in heart, peritoneal wall and aorta was measured after injection of 50 µg of LPS intraperitoneally with or without 200 µg of OxPAPC in 0.9% saline. After 3 h, animals were killed, and the tissues were processed for E-selectin mRNA quantification. **g**, OxPAPC inhibits LPS-induced extravasation of white blood cells into the peritoneum. **h**, OxPAPC inhibits LPS-induced oedema formation in the peritoneal wall. Staining is with haematoxylin–eosin. Arrowheads indicate inflammatory cells. **i**, OxPAPC increases survival in mice treated with lethal doses of LPS. **a–i**, See Methods for experimental details.

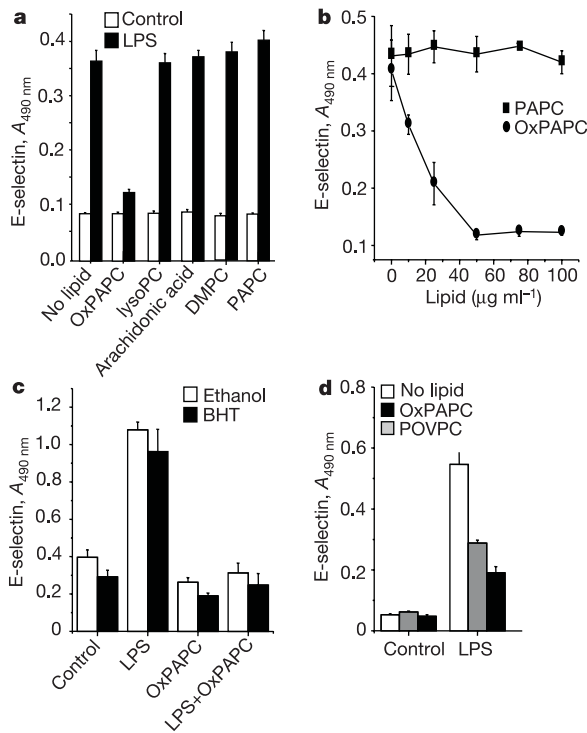


Figure 4 The anti-endotoxin activity of OxPAPC is not mimicked by other lipids, crucially depends on OxPAPC oxidation, and is not mediated by free radicals. **a**, The inhibitory effect of OxPAPC is not mimicked by other lipids. HUVEC were incubated with the indicated lipids ($30 \mu\text{g ml}^{-1}$) and 300 ng ml^{-1} LPS. **b**, Oxidation of PAPC is a prerequisite for its anti-endotoxin activity. HUVEC were treated with indicated concentrations of sonicated native or oxidized PAPC and 300 ng ml^{-1} LPS. **c**, Inhibitory action of OxPAPC is not rescued by the free-radical scavenger butylated hydroxytoluene (BHT). HUVEC were stimulated with LPS/OxPAPC in the presence of $25 \mu\text{M}$ BHT or 0.1% ethanol (vehicle). **d**, POVPC inhibits LPS-induced upregulation of E-selectin. HUVEC were treated with POVPC or OxPAPC (each at $20 \mu\text{g ml}^{-1}$) and LPS (300 ng ml^{-1}). **a-d**, After 4 h, surface expression of E-selectin was determined by cell ELISA as described in Methods.

biological effects, namely arachidonic acid and lysophosphatidylcholine, did not inhibit LPS-induced upregulation of E-selectin (Fig. 4a). Furthermore, only oxidized PAPC possessed the inhibitory activity, while non-oxidized PAPC or phosphatidylcholine containing saturated fatty acids (dimyristoylphosphatidylcholine, DMPC) were inactive (Fig. 4a and b). These data clearly show that oxidative modification is essential for phospholipids to gain anti-endotoxin activity. The inhibitory activity was not due to free-radical generation or free radicals already present in the OxPAPC preparations because addition of the antioxidant butylated hydroxytoluene had no effect (Fig. 4c). To identify individual lipid oxidation products responsible for the inhibitory activity, the lipid oxidation products contained in OxPAPC were fractionated using high-performance liquid chromatography/mass spectrometry (HPLC/MS)⁹. In fractions that inhibited LPS action, we consistently found a molecule with mass-to-charge ratio (m/z) = 594, previously identified as 1-palmitoyl-2-oxovalerolyl-*sn*-glycero-3-phosphorylcholine (POVPC)⁹. In fact, synthesized POVPC⁸ inhibited LPS-induced E-selectin expression (Fig. 4d).

To determine whether OxPAPC exerts inhibitory effects also *in vivo*, we investigated LPS-induced inflammation at various levels of the inflammatory response, that is, NF κ B activation, expression of inflammatory adhesion molecules and extravasation of inflammatory cells, using three established models of local and systemic LPS-induced inflammation in mice. In a skin model, OxPAPC inhibited LPS-induced accumulation of myeloperoxidase-expressing leuko-

cytes at the site of injection (Fig. 3a, b). In an air pouch model²³, OxPAPC inhibited LPS-induced neutrophil immigration into the pouch cavity (Fig. 3c), p65 nuclear translocation in cells of the pouch wall (Fig. 3d) and VCAM-1 expression in endothelial cells as well as myofibroblasts in the pouch wall (Fig. 3e). After intraperitoneal injection of LPS, OxPAPC inhibited induction of E-selectin messenger RNA locally in the peritoneal wall, but also systemically in heart and aorta (Fig. 3f). Moreover, OxPAPC inhibited accumulation of blood-borne cells in the peritoneal cavity (Fig. 3g) and blocked oedema formation in the subserosal layer of the peritoneal wall (Fig. 3h). These data show that OxPAPC inhibits inflammatory effects of LPS also *in vivo*. Finally, OxPAPC significantly increased survival in mice injected with lethal doses of LPS (Fig. 3i).

Taken together, these results demonstrate that inhibition of LPS-induced acute inflammation by oxidized phospholipids suppresses innate immune responses both *in vitro* and *in vivo*. Our data clearly show that the anti-inflammatory action of OxPAPC is specific for LPS as compared to inflammatory cytokines TNF α and IL-1 β . Thus, endogenously formed oxidized phospholipids potentially blunt the initiation of LPS-induced acute inflammation, although previous data indicate that they propagate chronic inflammation⁷. Furthermore, OxPAPC inhibits action of endotoxin through a mechanism apparently different from simple LPS entrapment leading to the formation of biologically inactive complexes. Our data instead suggest that the inhibition of the LPS effects by OxPAPC is mediated by interference with LPS binding to LBP and CD14, thereby inhibiting LPS presentation to TLR4.

We also find that oxidation is crucial for PAPC to acquire the anti-endotoxin activity. Thus, oxidation renders phospholipids capable of interacting with components of the innate immune system and of modifying responses to Gram-negative bacterial products. Given that under normal conditions LPS antagonistic activity of PAPC is low, it may increase dramatically at sites of bacterial inflammation owing to high concentrations of neutrophil-derived reactive oxygen species inducing lipid peroxidation⁵. This raises the possibility that phospholipid oxidation serves as a negative feedback mechanism to downregulate acute inflammation in Gram-negative infection. In addition, we identify POVPC as one chemical structure exerting anti-endotoxin effects, a compound quite different from previously described LPS scavengers or LPS receptor antagonists such as polymyxin B or lipid-A like substances^{15,16}. These findings open up the possibility of developing new anti-endotoxin drugs with distinct chemical and pharmacodynamic properties. □

Methods

Lipids and lipopolysaccharide

PAPC, DMPC, 1-palmitoyl-*sn*-glycero-3-phosphorylcholine (lysoPC), arachidonic acid and lipopolysaccharide from *E. coli* serotype 055:B5 were purchased from Sigma-Aldrich, Vienna, Austria. OxPAPC was obtained by air oxidation of dry PAPC as described previously⁹ and was stored in chloroform at -70°C . POVPC was synthesized as described⁸. Immediately before the experiment, lipids were dried in glass tubes under the stream of N_2 and solubilized in culture medium by vigorous vortexing for 30 s. Where indicated, the lipids were additionally sonicated for 30 s.

Cells

Human umbilical-vein endothelial cells (HUVEC) were obtained and cultured as described¹⁰. Monolayers of HUVEC at passages 3 to 6 were treated with OxPAPC and agonists in medium 199 containing 10% supplemented calf serum or fetal calf serum (FCS) (HyClone). OxPAPC and other lipids were added to cells 20 min before the addition of stimuli. Longer preincubation did not produce stronger inhibition of the effects of LPS. In the absence of serum, the cells were insensitive to LPS.

Cell ELISA

For the enzyme-linked immunosorbent assay (ELISA), HUVEC were treated with lipids and agonists for 4 h, and then the cells were washed and fixed. Cell-surface-expressed E-selectin, ICAM-1 or VCAM-1 was detected using corresponding antibodies (R&D

Systems), secondary peroxidase-conjugated antibodies and *o*-phenylenediamine as substrate.

Quantification of NFκB-dependent transcription

Co-transfection of HUVEC with pNFκB-Luc (Stratagene) and pCMVβ (Clontech) was performed as described¹⁰. Two days after transfection, the cells were stimulated with 300 ng ml⁻¹ LPS in the presence or absence of OxPAPC, and 6 h later were processed for luciferase and β-galactosidase activity measurements.

Analysis of p65/DNA binding

HUVEC were stimulated with 300 ng ml⁻¹ LPS for 60 min in the presence or absence of 25 μg ml⁻¹ OxPAPC. Analysis of p65 binding to its consensus oligonucleotide was performed in HUVEC lysates using the ELISA-based Trans-AM NFκB p65 kit (Active Motif).

Western blotting

HUVEC were stimulated with 300 ng ml⁻¹ LPS or 20 U ml⁻¹ TNFα in the presence or absence of 50 μg ml⁻¹ OxPAPC. After 20 min (phospho-IκBα), 1 h (total IκBα) or 2 h (p38 MAPK), cells were scraped and analysed by western blotting as described¹⁰.

Limulus amoebocyte lysate assay

OxPAPC aliquots (60 μg ml⁻¹) were mixed with equal volumes of LPS dilutions to produce final concentrations indicated on the x-axis in Fig. 2b. After 5 min at 37 °C, LAL reagent was added and LAL activity was determined by a quantitative chromogenic assay (Endochrome, Charles River Endosafe).

Binding of biotin-LPS to CD14 and LBP

LPS was biotinylated using EZ-Link Biotin-LC-Hydrazide (Pierce). Binding of biotin-LPS to recombinant human CD14 (Biometec) adsorbed onto ELISA plates was measured as described in ref. 24. Binding reaction was performed for 30 min at 37 °C in PBS/0.5% BSA buffer containing 1% FCS. In the absence of serum, binding of biotin-LPS to CD14 was below the detection limit. Bound biotin-LPS was detected with streptavidin-peroxidase and *o*-phenylenediamine. Binding of biotin-LPS to recombinant LBP (Biometec) captured by anti-LBP (HM14, a gift from W. A. Buurman) adsorbed to ELISA plates was measured as described in ref. 25. The binding was performed in PBS/0.1% BSA buffer. Detection of bound biotin-LPS was performed as described for CD14.

Animals

Experiments were performed according to Austrian animal rights law using female C57BL/6J mice (Institut für Labortierkunde und -genetik) of 20 g body weight.

Skin model of inflammation

LPS (10 μg) with or without OxPAPC (50 μg) in the final volume of 50 μl of 0.9% saline was injected intradermally into the abdominal region. After 24 h, mice were killed, and the skin at the injection site was excised and either embedded in optimal-cutting-temperature compound for immunohistochemistry or homogenized in potassium phosphate buffer (50 mM, pH 6.0) containing 0.5% hexadecyltrimethylammonium bromide. Sections of skin were stained for myeloperoxidase (MPO) using anti-MPO (from Dako) and Alexa 466-labelled secondary antibodies (Molecular Probes). Nuclei were stained with DAPI (Sigma-Aldrich). MPO activity in homogenates was monitored at 460 nm using H₂O₂ and *o*-dianisidine (Sigma-Aldrich) as substrates²⁶.

Air pouch model of inflammation

Air pouches of 5 ml were raised on day 0 on the dorsal surface of mice under light halothane anaesthesia, and a further 3 ml of air was injected 3 days later²⁷. At day seven, 50 μg of LPS, 250 μg of OxPAPC, or a combination of both, was injected into the pouch in 1 ml of 0.9% saline. Twenty-four hours later, mice were killed, the pouches were lavaged and leukocytes were counted. Sections of air pouch wall were stained for p65 (Santa Cruz Biotechnology) or VCAM-1 (Southern Biotechnology Associates). Nuclei were stained with DAPI.

Peritoneal model of inflammation

Mice were injected intraperitoneally (i.p.) with 10 μg of LPS with or without 50 μg of OxPAPC at days 0 and 1. At day 2, the animals were killed and peritoneal leukocytes were counted in the lavage fluid. Paraffin-embedded sagittal sections of the anterior abdominal wall were stained with haematoxylin and eosin.

Survival studies

Mice were injected i.p. with 0.6 mg of LPS with or without 1.2 mg of OxPAPC in 0.5 ml of 0.9% saline. Survival was checked three times daily for up to 5 days.

mRNA expression

The mice were killed, and isolated organs were immersed into the RNAlater solution (Ambion). One μg of total RNA isolated using the RNAqueous 4PCR kit (Ambion) was reverse transcribed using GeneAmp RNA PCR core kit (Applied Biosystems).

Quantification of E-selectin mRNA was performed by real-time polymerase chain reaction (PCR) using the LightCycler instrument and Fast Start DNA Master SYBR Green I kit (Roche Diagnostics) as recommended by the manufacturer. The following primers were used: forward, 5'-GGTTGGTGAGGTGTGCTC; reverse, 5'-TGATCTTTCCCGGAAC TGC. Each sample was also analysed for expression of β₂-microglobulin, which was used for normalization of E-selectin data.

Statistics

The data are presented as mean values ± standard deviations. The data are representative of at least two experiments producing similar results.

Received 30 May; accepted 10 July 2002; doi:10.1038/nature01023.

1. Medzhitov, R. Toll-like receptors and innate immunity. *Nature Rev. Immunol.* **1**, 135–145 (2001).
2. Aderem, A. & Ulevitch, R. J. Toll-like receptors in the induction of the innate immune response. *Nature* **406**, 782–787 (2000).
3. Chow, J. C., Young, D. W., Golenbock, D. T., Christ, W. J. & Gusovsky, F. Toll-like receptor-4 mediates lipopolysaccharide-induced signal transduction. *J. Biol. Chem.* **274**, 10689–10692 (1999).
4. Beutler, B. Tlr4: central component of the sole mammalian LPS sensor. *Curr. Opin. Immunol.* **12**, 20–26 (2000).
5. Hampton, M. B., Kettle, A. J. & Winterbourn, C. C. Inside the neutrophil phagosome: oxidants, myeloperoxidase, and bacterial killing. *Blood* **92**, 3007–3017 (1998).
6. Zhang, R., Shen, Z., Nauseef, W. M. & Hazen, S. L. Defects in leukocyte-mediated initiation of lipid peroxidation in plasma as studied in myeloperoxidase-deficient subjects: systematic identification of multiple endogenous diffusible substrates for myeloperoxidase in plasma. *Blood* **99**, 1802–1810 (2002).
7. Lusis, A. J. Atherosclerosis. *Nature* **407**, 233–241 (2000).
8. Leitinger, N. *et al.* Structurally similar oxidized phospholipids differentially regulate endothelial binding of monocytes and neutrophils. *Proc. Natl Acad. Sci. USA* **96**, 12010–12015 (1999).
9. Watson, A. D. *et al.* Structural identification by mass spectrometry of oxidized phospholipids in minimally oxidized low density lipoprotein that induce monocyte/endothelial interactions and evidence for their presence *in vivo*. *J. Biol. Chem.* **272**, 13597–13607 (1997).
10. Bochkov, V. N. *et al.* Oxidized phospholipids stimulate tissue factor expression in human endothelial cells via activation of ERK/EGR-1 and Ca⁺⁺/NFAT. *Blood* **99**, 199–206 (2002).
11. Elass-Rochard, E. *et al.* Lactoferrin inhibits the endotoxin interaction with CD14 by competition with the lipopolysaccharide-binding protein. *Infect. Immun.* **66**, 486–491 (1998).
12. Emancipator, K., Csako, G. & Elin, R. J. *In vitro* inactivation of bacterial endotoxin by human lipoproteins and apolipoproteins. *Infect. Immun.* **60**, 596–601 (1992).
13. Kitchens, R. L., Thompson, P. A., Viriyakosol, S., O'Keefe, G. E. & Munford, R. S. Plasma CD14 decreases monocyte responses to LPS by transferring cell-bound LPS to plasma lipoproteins. *J. Clin. Invest.* **108**, 485–493 (2001).
14. Wurfel, M. M. & Wright, S. D. Lipopolysaccharide-binding protein and soluble CD14 transfer lipopolysaccharide to phospholipid bilayers: preferential interaction with particular classes of lipid. *J. Immunol.* **158**, 3925–3934 (1997).
15. Rustici, A. *et al.* Molecular mapping and detoxification of the lipid A binding site by synthetic peptides. *Science* **259**, 361–365 (1993).
16. Christ, W. J. *et al.* E5531, a pure endotoxin antagonist of high potency. *Science* **268**, 80–83 (1995).
17. Golenbock, D. T., Hampton, R. Y., Qureshi, N., Takayama, K. & Raetz, C. R. Lipid A-like molecules that antagonize the effects of endotoxins on human monocytes. *J. Biol. Chem.* **266**, 19490–19498 (1991).
18. Tanamoto, K. & Azumi, S. Salmonella-type heptaacylated lipid A is inactive and acts as an antagonist of lipopolysaccharide action on human line cells. *J. Immunol.* **164**, 3149–3156 (2000).
19. Frey, E. A. *et al.* Soluble CD14 participates in the response of cells to lipopolysaccharide. *J. Exp. Med.* **176**, 1665–1671 (1992).
20. Su, G. L., Simmons, R. L. & Wang, S. C. Lipopolysaccharide binding protein participation in cellular activation by LPS. *Crit. Rev. Immunol.* **15**, 201–214 (1995).
21. Sugiyama, T. & Wright, S. D. Soluble CD14 mediates efflux of phospholipids from cells. *J. Immunol.* **166**, 826–831 (2001).
22. Yu, B., Hailman, E. & Wright, S. D. Lipopolysaccharide binding protein and soluble CD14 catalyze exchange of phospholipids. *J. Clin. Invest.* **99**, 315–324 (1997).
23. Lawrence, T., Gilroy, D. W., Colville-Nash, P. R. & Willoughby, D. A. Possible new role for NF-κB in the resolution of inflammation. *Nature Med.* **7**, 1291–1297 (2001).
24. Cunningham, M. D. *et al.* *Helicobacter pylori* and *Porphyromonas gingivalis* lipopolysaccharides are poorly transferred to recombinant soluble CD14. *Infect. Immun.* **64**, 3601–3608 (1996).
25. Scott, M. G., Vreugdenhil, A. C., Buurman, W. A., Hancock, R. E. & Gold, M. R. Cutting edge: cationic antimicrobial peptides block the binding of lipopolysaccharide (LPS) to LPS binding protein. *J. Immunol.* **164**, 549–553 (2000).
26. Bradley, P. P., Priebe, D. A., Christensen, R. D. & Rothstein, G. Measurement of cutaneous inflammation: estimation of neutrophil content with an enzyme marker. *J. Invest. Dermatol.* **78**, 206–209 (1982).

Acknowledgements

This project was funded by the Austrian Science Foundation and by the ICP Program of the Austrian Federal Ministry for Education, Science and Culture.

Competing interests statement

The authors declare that they have no competing financial interests.

Correspondence and requests for materials should be addressed to N.L. (e-mail: norbert.leitinger@univie.ac.at).